



ELSEVIER

Contents lists available at ScienceDirect

Bioorganic & Medicinal Chemistry Letters

journal homepage: www.elsevier.com/locate/bmclSynthesis and evaluation of *N*-(4-benzylphenyl)piperazines as VGF inducers

Tetsuya Toba^{a,b,*}, Ryosuke Suzuki^{a,c}, Junko Futamura-Takahashi^d, Yoshito Kawamoto^b, Shigeki Tamura^b, Mariko Kuroda^b, Yoshiari Shimmyo^e, Michinori Kadokura^b, Kazumichi Goto^b, Teruyoshi Inoue^c, Tsuyoshi Muto^b, Hirokazu Annoura^b

Asubio Pharma Co., Ltd., 6-4-3 Minatojima-Minamimachi, Chuo-ku, Kobe 650-0047, Japan

ARTICLE INFO

Keywords:

VGF inducer
Cytoprotection
Structure-activity relationship
SUN N8075
SH-SY5Y

ABSTRACT

A series of compounds was discovered that induce the production of VGF mRNA in SH-SY5Y cells and exhibit cytoprotection under tunicamycin induced endoplasmic reticulum (ER) stress. The aminophenol ring and linker chain of the template SUN N8075 (**1**) was modified to yield compounds with higher efficacy and lower propensity for adverse effects.

VGF (non-acronymic) is a neuropeptide precursor whose proteolysis fragments are involved in a variety of functions including the regulation of energy homeostasis, reproductive mechanisms, synaptic plasticity, and neuronal apoptosis.¹ Among its myriad of functions, VGF has attracted attention for its involvement in amyotrophic lateral sclerosis (ALS), a fatal progressive neurodegenerative disorder affecting motor neurons which eventually results in respiratory deficiency. VGF levels are reduced in the plasma and fibroblasts² of ALS patients, as well as in cerebrospinal fluid (CSF) which are in parallel with development of ALS symptoms.³ The Hara group reported that VGF depletion participates in the onset and/or progression of ALS.⁴ VGF gene expression can be induced by neurotrophins such as nerve growth factor (NGF),⁵ brain-derived neurotrophic factor (BDNF),⁶ and neurotrophin-3 (NT3),⁷ but to the best of our knowledge, SUN N8075 (**1**)⁴ and clioquinol (**2**)⁸ are the only small-molecule inducers of VGF reported to date (Fig. 1). Compound **1**, a dual Na⁺/Ca²⁺ channel blocker and antioxidant,⁹ induces the production of VGF peptides, rescues human neuroblastoma (SH-SY5Y) cells from tunicamycin induced endoplasmic reticulum (ER) stress, and prolongs the life span of *in vivo* mouse ALS models with SOD1 mutation.⁴ Although **1** is an attractive candidate for the ALS therapy, it contains the chemically and biologically unstable *p*-aminophenol moiety. Drugs containing aminophenol often exhibit hepatotoxicity,^{10–13} and this structure is a known substrate that can cause mechanism-based inactivation (MBI) of CYP450 enzymes,¹¹ possibly

leading to adverse drug-drug interactions.

Our goal was to discover novel compounds based on SUN N8075 scaffold with a refined profile. The effect of **1** on the survival of SOD1-G93A transgenic mice was comparable to that of riluzole,^{4,14,15} the only FDA-approved ALS treatment until the recent approval of Radicava® in 2017. Thus, the main objective of this study was to transform **1** into compounds with a reduced risk for adverse effects while retaining/augmenting its efficacy. In this letter, the syntheses of multiple derivatives of **1** as VGF inducers are disclosed, and their structure-activity relationship is discussed.

Compounds **5–8** were synthesized in a similar manner to **1**⁹ by coupling the intermediate epoxide **3** and 1-(4-(4-fluorobenzyl)phenyl)piperazine (**4**) in 2-propanol under reflux (Scheme 1). Compound **10** was synthesized by coupling **4** with intermediate **9** prepared from 6-hydroxyquinoline and 1,3-dibromopropane. Compounds **18–27** with a fluorinated linker were prepared as shown in Scheme 2. The fluorinated malonic acid esters **11a** and **b** were reduced to their corresponding diols **12**, which were mono-protected with *tert*-butyl diphenyl silyl (TBDPS) group to afford **13**. The free hydroxy group of **13** was triflated and reacted with **4** to yield intermediate **15**, which were subsequently desilylated, triflated, and reacted with various aromatic hydroxy groups to afford target compounds **18–27**. The (*S*)-enantiomer of **23** was prepared from commercially available (*S*)-glycidyl trityl ether (**29**) (Scheme 3). Compounds **28** and **29** were heated to give a propanetriol

* Corresponding author.

E-mail address: toba.tetsuya.zh@daiichisankyo.co.jp (T. Toba).

^a These authors contributed equally to this work.

^b Present address: Shinagawa R&D Center, Daiichi Sankyo Co., Ltd., Tokyo 140-8710, Japan.

^c Present address: Head Office, Daiichi Sankyo Co., Ltd., Tokyo 103-8426, Japan.

^d Deceased, September 14, 2017. This paper is dedicated to the memory of Ms. Junko Futamura-Takahashi.

^e Present address: Shonan Research Center, Takeda Pharmaceutical Co., Ltd., Kanagawa 251-8555, Japan.

<https://doi.org/10.1016/j.bmcl.2018.05.047>

Received 29 March 2018; Received in revised form 23 May 2018; Accepted 24 May 2018
0960-894X/© 2018 Elsevier Ltd. All rights reserved.

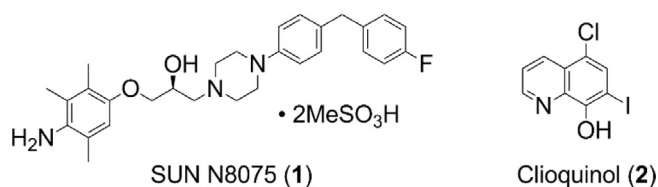
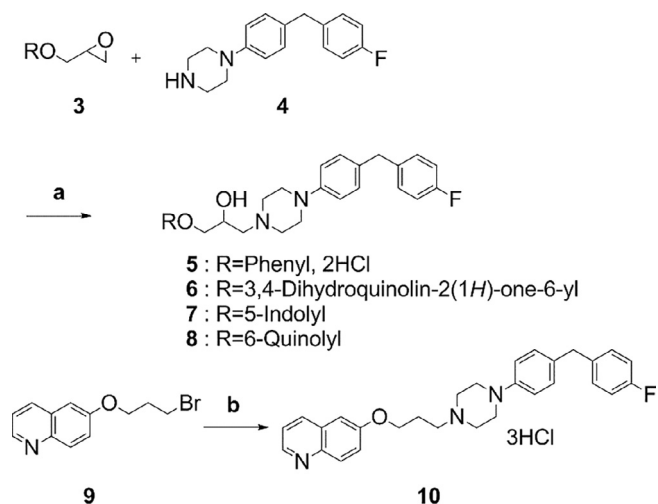
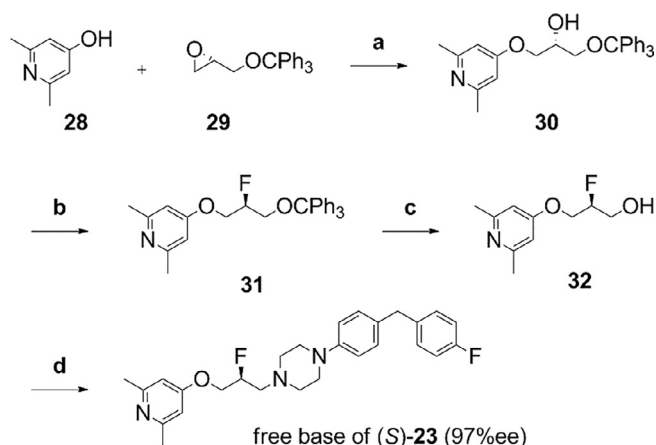


Fig. 1. Structures of known VGF inducers.

Scheme 1. Reagents and conditions: (a) 2-PrOH, 50 °C to reflux, 19% (6), 70% (7), 79% (8), then 4 N HCl/dioxane for 5, 81%; (b) 4, K₂CO₃, DMF, rt, then 4 N HCl/EtOAc, 86%.

derivative **30**, which was deoxyfluorinated with Deoxo-Fluor®. Detritylation followed by triflation and coupling with **4** yielded the free base of (*S*)-**23** in a 97% ee. The enantiomer (*R*)-**23** was prepared along with (*S*)-**23** by the HPLC resolution of racemic **23** (free base) using CHIRAL-PAK® IC column. The stereochemistry was determined by comparing retention times with (*S*)-**23** prepared as above.

The analogs prepared were evaluated *in vitro* for their VGF mRNA induction capabilities by quantitative real-time PCR¹⁶ in parallel with cytoprotection under tunicamycin induced ER stress in SH-SY5Y cells.¹⁷ The MBI risk was evaluated by the ratio of metabolite formation of testosterone (a probe substrate for CYP3A4) after preincubation of the

Scheme 3. Reagents and conditions: (a) K₂CO₃, EtOH, reflux, 45%; (b) Deoxo-Fluor®, CH₂Cl₂, rt; (c) TFA, CH₂Cl₂, rt, 80% (2 steps); (d) i: Tf₂O, iPr₂NEt, CH₂Cl₂, -78 to -20 °C, ii: 4, CH₂Cl₂, rt, 80%.

human liver microsomes and test compounds with and without NADPH.¹⁸ Their difference shows the degree of inactivation by the metabolized test compound during preincubation, proceeding only in the presence of NADPH. Since MBI is caused by reactive metabolite formation at the active site of CYP450, metabolic stability towards human liver microsomes (HLMs) *in vitro* was also evaluated.¹⁹ In the cell-based VGF mRNA induction and cytoprotection assays, the efficacy of test compounds was normalized to that of **1**. For the cytoprotection assay, the mean viability of tunicamycin-treated cells throughout the study was 45% (standard deviation [SD] 6.6%) of untreated control cells, and the mean viability with additional treatment of **1** at 3 μM was 82% (SD 11%) of untreated controls. The protection from tunicamycin treatment by the reference compound **1** was defined 100%, and those by the test compounds were expressed as the ratio to **1**. For the VGF induction assay, mean increase in VGF mRNA throughout the study by **1** at 3 μM was 5.1-fold (SD 2.8) over untreated control. The results are listed in Table 1.

Compound **1** showed low metabolic stability and moderate risk of MBI in the CYP450 assay. Compound **5** with an unsubstituted phenyl ring exhibited a marked decrease in VGF induction. Together with the complete loss of action with the truncation of the phenyl ring (not shown), an aromatic ring and polar functional group were both

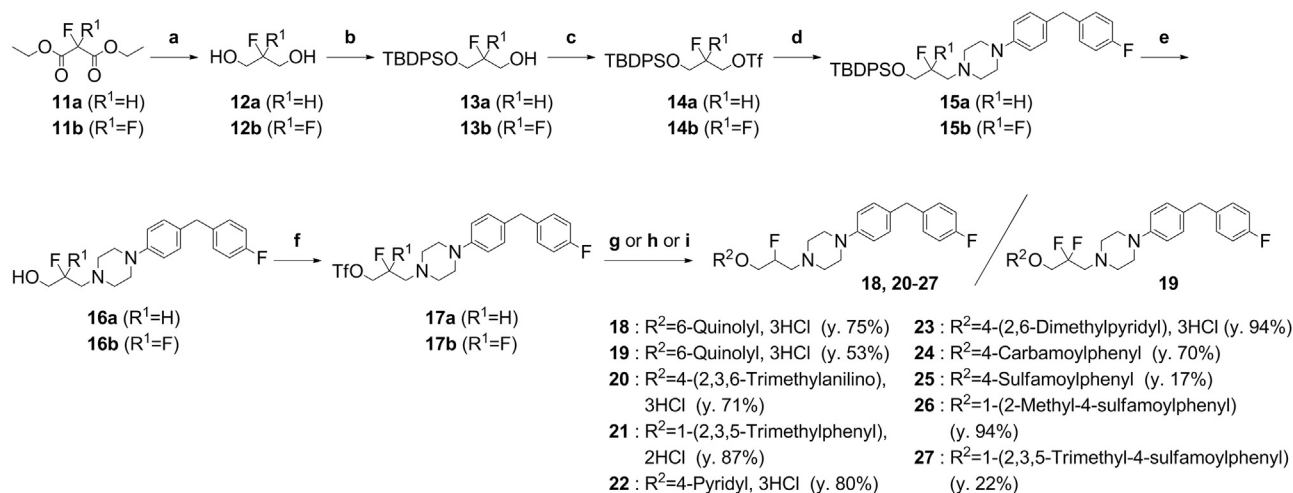
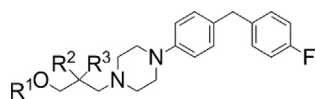
Scheme 2. Reagents and conditions: (a) NaBH₄, THF, 50% aq. EtOH, 0 °C to rt, 85% (**12a**), 44% (**12b**); (b) NaH, TBDPSCI, THF, 0 °C to rt, 52% (**13a**), 51% (**13b**); (c) Tf₂O, iPr₂NEt, CH₂Cl₂, -70 to -20 °C; (d) 4, iPr₂NEt, DMF, 80 °C, 53% (**15a**, 2 steps), 83% (**15b**, 2 steps); (e) TBAF, THF, rt, 86% (**16a**), 87% (**16b**); (f) Tf₂O, iPr₂NEt, CH₂Cl₂, -65 to -30 °C, 92% (**17a**); (g) R²OH, K₂CO₃, DMF, rt, 17–94%; (h) R²OH, Cs₂CO₃, DMF, 0 °C to rt, then 4 N HCl/EtOAc, CHCl₃, 53–94%; (i) R²OH, Cs₂CO₃, DMF, rt, then TFA, CH₂Cl₂, rt, then 4 N HCl/EtOAc, CHCl₃, 71%.

Table 1
VGF induction, cytoprotection, MBI risk and metabolic stability of compounds **1**, **5–8**, **10**, and **18–19**.



Compound	R ¹	R ²	R ³	VGF induction (%) ^a Mean ± SD	Cell viability (%) ^a Mean ± SD	MBI index ^b (% remaining)	Metabolic rate (pmol/min/mg protein)
1 ^c		OH	H	(100)	(100)	57	153
5 ^d		OH	H	8 ± 26	43 ± 11	NT ^e	28
6		OH	H	32 ± 41	33 ± 12	88	27
7		OH	H	30 ± 41	43 ± 8	59	79
8		OH	H	36 ± 21	64 ± 27	70	122
10 ^d		H	H	52 ± 10	75 ± 7	94	47
18 ^d		F	H	77 ± 8	89 ± 6	82	79
19 ^d		F	F	68 ± 31	67 ± 13	93	34

^a At 3 μM, in reference to **1**.

^b The remaining activity of CYP3A4 after preincubation with the test compound and NADPH.

^c MsOH salt.

^d HCl salt.

^e NT: Not tested.

assumed to be essential for proper function. Among the several heteroatom-bearing aromatic derivatives, quinoline derivative **8** showed moderate efficacy in VGF induction and cytoprotection. Removal of the hydroxy group in the linker retained the activity, showed improved stability, and decreased the risk for MBI (compound **10**). Substitution of the hydroxy group with a fluorine atom led to further potentiation (compound **18**). Addition of another fluorine, to form *gem*-difluoro compound **19**, showed good stability comparable to the non-substituted linker, but was not as effective as **18** in the induction of VGF.

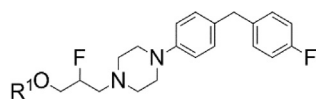
The potential of aromatic ring derivatization was further investigated with the monofluoride linker (Table 2). The aminophenol ring same as **1** showed a similar but slightly improved profile (compound **20**). Although the trimethylphenyl ring without the amino group resulted in decreased efficacy, the MBI risk became negligible, indicating that the *p*-aminophenol ring is primarily responsible for the MBI risk (compound **21**). The dimethylpyridine analog **23** showed comparable activity towards VGF induction to the quinoline derivative **18**, while analog **22** with unsubstituted pyridine showed negligible induction. Although **22** lost its activity, its metabolic stability was significantly improved, indicating that the methyl group on the ring is another metabolic site. Enantiomeric (*R*)-**23** and (*S*)-**23** showed similar profiles when racemic **23** was optically resolved, but the metabolic stability of (*S*)-**23** was somewhat higher than that of (*R*)-**23**. Benzenesulfonamide (**25**) but not benzamide (**24**) was effective as a surrogate for the quinoline ring and exhibited sufficient stability. The monomethylated benzenesulfonamide derivative **26** showed a marked enhancement in VGF induction/cytoprotection equipotent to **1**, with greatly improved metabolic stability and negligible MBI risk. The

trimethyl derivative **27** was found to be the most potent VGF inducer exceeding the level of **1**.

It should be noted that VGF induction and cytoprotective activity increased in a somewhat parallel manner. The expression of VGF represents the major mechanism of action of **1** as indicated by siRNA experiments.⁴ From the result presented herein it is reasonable to assume that the VGF induction in this series contributes to the neuronal cell protection under ER stress. On the other hand, even the cytoprotection of the most potent compounds did not exceed that of **1**. Cytoprotection by **1** has likely reached the maximum level detectable by the assay used in this study, presumably with the participation of other mechanisms.

In conclusion, we prepared a series of compounds that induce VGF mRNA production in SH-SY5Y cells. The compounds showed near-parallel protection of the SH-SY5Y cells under tunicamycin induced ER stress. The *p*-aminophenol ring in **1** was shown to be responsible for the MBI risk, but the aromatic ring and polar functional group(s) were determined to be necessary for the efficacy of the drug. The methyl group on the phenyl ring is one of the main metabolic site, but has a positive effect on cell protection. Removal of the hydroxy group on the linker or substitution with a fluorine atom led to further potentiation and ameliorated the MBI risk. Through the modification of the aminophenol ring and linker chain in **1**, compounds such as **27**²⁰ were obtained with higher efficacy and a reduced propensity for hepatotoxicity and/or drug-drug interaction. Further structural optimization of these VGF inducers including the diphenylmethyl moiety is underway, and will be reported in due course.

Table 2
VGF induction, cytoprotection, MBI risk and metabolic stability of compounds 20–27.



Compound	R ¹	VGF induction (%) ^a Mean ± SD	Cell viability (%) ^a Mean ± SD	MBI index ^b (% remaining)	Metabolic rate (pmol/min/mg protein)
20 ^c		126 ± 9	94 ± 9	75	106
21 ^c		75 ± 13	60 ± 7	107	25
22 ^c		13 ± 12	13 ± 5	101	< 10
23 ^c		79 ± 10	82 ± 8	67	41
(R)-23 ^c		78 ± 14	93 ± 27	83	71
(S)-23 ^c		68 ± 25	96 ± 13	80	37
24		20 ± 5	21 ± 5	76	34
25		71 ± 28	88 ± 10	99	12
26		114 ± 16	105 ± 14	108	17
27		172 ± 13	106 ± 15	92	32

^a At 3 μM, in reference to 1.

^b The remaining activity of CYP3A4 after preincubation with the test compound and NADPH.

^c HCl salt.

Acknowledgements

The authors would like to thank Ms. S. Kanki-Mekata and Mr. T. Tabata for performing metabolic stability assays. Drs. Y. Minamitake, T. Nishihara, Y. Kita, H. Ogasawara, Y. Fukuda, A. Ogata, and M. Hasegawa are acknowledged for valuable discussions and support throughout this study.

A. Supplementary data

Supplementary data associated with this article can be found, in the online version, at <http://dx.doi.org/10.1016/j.bmcl.2018.05.047>.

References

1. Ferri GL, Noli B, Brancia C, D'Amato F, Cocco C. *J Chem Neuroanat.* 2011;42:249–261 and references cited therein.
2. Brancia C, Noli B, Boido M, et al. *PLoS One.* 2016;11:e0164689.
3. Zhao Z, Lange DJ, Ho L, et al. *Int J Med Sci.* 2008;5:92–99.
4. Shimazawa M, Tanaka H, Ito Y, et al. *PLoS One.* 2010;5:e15307.
5. Levi A, Eldridge JD, Paterson BM. *Science.* 1985;229:393–395.
6. Alder J, Thakker-Varia S, Bangasser DA, et al. *J Neurosci.* 2003;23:10800–10808.
7. Eagleson KL, Fairfull LD, Salton SRJ, Levitt P. *J Neurosci.* 2001;21:9315–9324.
8. Katsuyama M, Ibi M, Matsumoto M, Iwata K, Ohshima Y, Yabe-Nishimura C. *J Pharmacol Sci.* 2014;124:427–432.
9. Annoura H, Nakanishi K, Toba T, et al. *J Med Chem.* 2000;43:3372–3376.
10. Vermeulen NPE, Bessems JGM, Van de Straat R. *Drug Metab Rev.* 1992;24:367–407.
11. Teng WC, Oh JW, New LS, et al. *Mol Pharmacol.* 2010;78:693–703.
12. Kalgutkar AS, Dalvie D, Obach RS, Smith DA. *Reactive drug metabolites.* John Wiley & Sons; 2012.
13. Ongarora DSB, Gut J, Rosenthal PJ, Masimirembwa CM, Chibale K. *Bioorg Med Chem Lett.* 2012;22:5046–5050.
14. Waibel S, Reuter A, Malessa S, Blaugrund E, Ludolph AC. *J Neurol.* 2004;251:1080–1084.
15. Del Signore SJ, Amante DJ, Kim J, et al. *Amyotroph Lateral Scler.* 2009;10:85–94.
16. *In vitro* VGF mRNA induction assay: To examine the effect of the SUN N8075 analog on VGF mRNA expression, SH-SY5Y cells were seeded in 12-well plates at a density of 2.0×10^5 cells per well. After the cells were incubated for 72 h, they were exposed to the various compounds at a concentration of 3 μM in DMEM/F12 with 1% FBS for 24 h. RNA was isolated using RNeasy mini kit (QIAGEN), cDNA was produced using QuantiTect Reverse Transcription Kit (QIAGEN), and quantitative real-time PCR was performed using the TaqMan Gene Expression Assay (VGF: Hs00705044-s1), TaqMan Gene Expression Master Mix (Thermo Fisher Scientific), and Mx3000P QPCR system (Agilent Technologies). Gene expression was normalized relative to the GAPDH internal control gene and assessed using the comparative C_T method.
17. *In vitro* cytoprotection assay: To assess the protective effect of the prepared compounds against ER stress-induced cell death, SH-SY5Y cells (ECACC) were suspended in Dulbecco's Modified Eagle Medium (DMEM, Thermo Fisher Scientific) containing 15% fetal bovine serum (FBS, EQUITECH-BIO), and 50 U/mL of penicillin-

- streptomycin (Thermo Fisher Scientific). The cells were then cultured using a collagen type-1 coated 96-well plate (Greiner) at a density of 1×10^4 cells/well in 5% CO₂ incubated at 37 °C. After 24 h, the culture media were changed to DMEM containing 1% FBS and 50 U/mL of penicillin-streptomycin, then the prepared compounds were added to the cells at a final concentration of 1–10 μM. After incubation with the compounds for 1 h, the cells were treated with tunicamycin at a final concentration of 2 μg/mL. To assess cell viability, a 10% WST-8 solution was added to the cells and incubated for 4 h in a CO₂ incubator 48 h after the tunicamycin treatment. The O.D. absorbance was recorded at 450 nm with background absorbance at 650 nm using a SpectraMax (Molecular Devices) instrument. The inhibition of ER-stress induced cell death for each compound was calculated from the mean of at least three experiments.
18. MBI assay: A mixture of human liver microsomes (0.5 mg/mL) and 10 μM test compound was pre-incubated in phosphate buffer (pH 7.4) for 30 min at 37 °C with and without NADPH (1 mM). The mixture was then added to the assay buffer containing testosterone (a probe substrate of CYP3A4) and NADPH, and incubated for an additional 10 min at 37 °C. The reaction was quenched with acetonitrile, and the testosterone metabolite concentration was measured by liquid chromatography-tandem mass spectrometry (LC-MS/MS) to evaluate the remaining CYP3A4 activity. MBI was depicted as the ratio of metabolized testosterone after preincubation with NADPH to that measured without NADPH.
19. Metabolic stability assay: For the incubation of the mixtures containing 1 μM test compound, 0.2 mL of HLMs (0.5 mg of microsomal protein/mL) and phosphate buffer (pH 7.4) were prepared in a 96-well plate. Reactions were initiated by the addition of NADPH (final concentration of 1 mM) and kept in a shaking water bath at 37 °C. Reactions were terminated by adding 50 μL of the incubation mixture to 100 μL of acetonitrile containing 100 ng/mL of an antipurine internal standard. The sampling point for $t = 0$ min was taken immediately after NADPH addition, and additional samples were taken at 3, 10, and 30 min. The samples were subsequently centrifuged for 5 min at 3000 rpm to pellet the precipitated microsomal protein, and the supernatant was subjected to LC-MS/MS analysis without further treatment. The metabolic rate was calculated according to the following equation: Metabolic rate [pmol/min/mg protein] = $\{1000 [\text{nM}] - (\text{conc. of residual compound} [\text{nM}])\} / \text{reaction time} [\text{min}] / 0.5 [\text{mg protein}]$.
20. Analytical data for **27**: ¹H NMR (400MHz, CDCl₃) δ = 7.15–7.09 (m, 2H), 7.08–7.03 (m, 2H), 6.98–6.92 (m, 2H), 6.88–6.83 (m, 2H), 6.59 (s, 1H), 5.14–4.93 (m, 1H), 4.76 (s, 2H), 4.29–4.15 (m, 2H), 3.87 (s, 2H), 3.21–3.15 (m, 4H), 2.92–2.76 (m, 2H), 2.76–2.70 (m, 4H), 2.67 (s, 3H), 2.62 (s, 3H), 2.19 (s, 3H); HRMS (FAB) m/z calculated for C₂₉H₃₆F₂N₃O₃S⁺ 544.2440, observed 544.2438. See also [Supplementary Data](#) for the synthetic procedure.